

Cellular interactions of biodegradable nanorod arrays prepared by nondestructive extraction from nanoporous alumina

Silko Grimm,^{ae} Jaime Martín,^b Gema Rodriguez,^b Mar Fernández-Gutierrez,^c Klaus Mathwig,^a Ralf B. Wehrspohn,^{df} Ulrich Gösele,^a Julio San Roman,^b Carmen Mijangos^b and Martin Steinhart^{*e}

Received 15th December 2009, Accepted 2nd February 2010

First published as an Advance Article on the web 26th February 2010

DOI: 10.1039/b926432a

Biodegradable extracellular matrices (ECMs) consisting of mechanically stable arrays of aligned poly(lactide) nanorods (nanorod diameter \approx 200 nm; lattice constant \approx 500 nm) with areas up to 9 cm² were prepared by nondestructive extraction from recyclable self-ordered nanoporous alumina hard templates. Fibroblasts formed dense tissue layers on the heparin/gelatin activated nanorod arrays, showed excellent adhesion and exhibited a highly elongated morphology such as in natural tissue. The synthetic approach reported here combining advantages of top-down lithography (well-defined topography) and self-assembly (low costs, high throughput, feature size in the 100 nm range) may yield ECMs for biomedical applications. Remarkably, on microrod arrays with four times larger feature sizes the fibroblasts were significantly less elongated and their proliferation was strongly reduced.

Introduction

The structural and functional configurations of native extracellular matrices (ECMs) govern the growth of tissue in biological systems since cells recognize topography, morphology and chemical nature of the ECMs. The high-throughput fabrication of synthetic ECMs consisting of biodegradable materials that interact with cells in a well-defined way has emerged as a central challenge at the intersection of biomedicine and materials science.¹ Structural features on subcellular and even nanoscopic length scales strongly influence cell growth under natural as well as under artificial conditions.^{2,3} Whereas predictive understanding as to how these features influence cell growth is still premature, it has become clear that the cues belonging to this structural level largely guide preferential cell adhesion. Cells probe topography and morphology of their surroundings by means of a well-defined recognition mechanism mediated by the emission and growth of filopodia. The extension of these specific members is a clear indication of specific cell/matrix interaction and cell proliferation. The interplay of filopodia and nanoscopic features was shown to be of critical importance for the reactions of cells to ECMs and for cell adhesion. Dalby and co-workers reported that specific interactions between the filopodia of fibroblasts and 10 nm high nano-islands of polymeric substrates

patterned by polymer demixing occurred, and that cell/substrate contact points were found to be located at the tips of the filopodia.⁴ Fibroblasts cultured on arrays of cylindrical nanocolumns with a diameter of 100 nm and a height of 160 nm prepared by colloidal lithography produced a high number of filopodia that detected the nanocolumns and specifically interacted with them.⁵

Fabrics of electrospun polymer fibers have been investigated intensively as artificial ECMs^{6–10} but suffer from broad distributions of fiber diameters. Moreover, electrospun fibers are predominantly oriented parallel to the surface on which the cells are seeded so that the rational incorporation of cues for cell adhesion has remained challenging. This drawback can be overcome by configurations based on arrays of aligned rods oriented perpendicular to an underlying substrate, because cells can recognize the tips of the rods as contact points for adhesion. ECMs of this kind exhibiting well-defined long-range ordered topographies were made of silicon,^{11,12} epoxy-based polymers¹² and poly(dimethylsiloxane)^{13,14} by lithographic techniques such as photolithography or electron beam lithography. However, these top-down methods are associated with limitations regarding either attainable feature sizes or throughput and patternable area. Moreover, it is difficult to structure biodegradable materials in this way. Patterning thermoplastics or photocurable prepolymers by means of nanoimprint lithography has yielded ordered arrays of pillars consisting of polymers such as polystyrene,¹⁵ poly(ethylene glycol)¹⁶ and biodegradable poly(glycerol-co-sebacate)acrylate¹⁷ but suffers from limitations regarding aspect ratios and spatial density of the array elements. By adapting a synthetic approach to one-dimensional nanostructures introduced by Martin and co-workers,^{18,19} arrays of nanorods consisting of biocompatible and biodegradable polymers were obtained by using commercially available anodic aluminium oxide (AAO) filters containing disordered arrays of nanopores as shape-defining hard templates.²⁰ However, the use of disordered AAO filter membranes characterized by broad

^aMax Planck Institute of Microstructure Physics, Weinberg 2, D-06120 Halle, Germany

^bInstituto de Ciencia y Tecnología de Polímeros, CIBER-BBN, CSIC, Juan de la Cierva 3, 28006 Madrid, España

^cFacultad de Farmacia, UCM, Ciudad Universitaria s/n, 28040 Madrid, España

^dInstitute of Physics, University of Halle-Wittenberg, Heinrich-Damerow-Strasse 4, 06120 Halle, Germany

^eInstitute for Chemistry, University of Osnabrück, Barbarastrasse 7, D-46069 Osnabrück, Germany. E-mail: martin.steinhart@uni-osnabrueck.de; Fax: +49 541-9693324; Tel: +49 541-9692817

^fFraunhofer Institute for Mechanics of Materials, Walter-Hülse-Str. 1, D-06120 Halle

pore diameter distributions and partially ill-defined pore morphologies is associated with two drawbacks. First, insufficient robustness of the commercially available AAO filter membranes and their pronounced surface roughness impede nondestructive mechanical release of nanorods formed within their pores. Hence, the nanorods must be released in a wet-chemical etching step involving the dissolution of the AAO hard templates. The consumption of the AAO hard templates, the specific precautions regarding work safety and environmental compatibility required when corrosive etching solutions are used and their disposal in compliance with environmental and safety guidelines are obvious drawbacks for the upscaling of the template-based fabrication of ECMs. Secondly, nanorods in nanorod arrays may laterally collapse owing to adhesive forces acting between neighboring nanorods^{21,22} so that the arrays predominantly consist of bunches of condensed nanorods.²³ To prevent the nanorods from collapsing, their stiffness and the design of the arrays they constitute have to be optimized. Since the range of materials nanorods in biodegradable ECMs may consist of is limited to relatively soft polymers, it is, therefore, crucial to adjust the diameters and aspect ratios of the nanorods and the spacing between them. In case of disordered AAO filters, it is possible to adjust the length of the nanorods within a certain range *via* the infiltration time. However, the scattering of the nanorod lengths, the small spacing between them and the overall ill-defined geometry of the pore arrays may result in condensation of the nanorods and therefore in significant deterioration of the topographic properties of the nanorod arrays. Thus, it is still challenging to fabricate artificial ECMs consisting of biodegradable materials based rod arrays with well-defined and customized geometries for biomedical applications including, for example, wound healing and tissue repair. To this end, a synthetic approach to ECMs combining the advantages of top-down lithography (well-defined topography) and self-assembly (low costs, high throughput, feature size in the 100 nm range) needs to be developed.

Here we report the economic fabrication of ordered arrays of aligned nanorods 180 nm in diameter consisting of the biodegradable polymer poly-DL-lactide (PDLLA). The PDLLA rod arrays obtained by nondestructive mechanical extraction from nanoporous self-ordered AAO^{24,25} serving as recyclable shape-defining hard templates had areas up to 9 cm². While the

throughput is comparable, the fabrication of artificial ECMs by means of recyclable AAO hard templates has several potential advantages over state-of-the-art top-down methods, such as nanoimprint lithography. First, limitations regarding the reduction of array periods and rod diameters to the sub-100 nm range can, in principle, be overcome since self-ordered AAO with corresponding feature sizes is readily available. The hard templates are thermally stable in the temperature range relevant to the processing of polymers. Therefore, mesoscopic structure formation processes such as crystallization²⁶ and phase separation,¹⁹ which affect the mechanical properties of the rods and their ability to release incorporated drugs in a controlled manner,²⁰ can be controlled by application of specific temperature profiles. We studied the cellular interactions of fibroblasts with the PDLLA nanorod arrays, because fibroblasts can be considered as a representative model system for global cell behavior. Dense layers of locally aligned fibroblasts with excellent viability and likewise excellent morphological properties were thus obtained. The fibroblasts, which possessed highly elongated shapes such as in their natural environment, recognized the nanorod arrays as rough surface providing nanorod tips as cues for cell adhesion, which were sensed by massively emitted filopodia. On microrod arrays fabricated by means of macroporous silicon²⁷ hard templates with feature sizes four times larger than those of PDLLA nanorod arrays extracted from AAO, the fibroblasts were significantly less elongated and their proliferation was strongly reduced.

Results and discussions

Fabrication of PDLLA nanorod arrays by nondestructive extraction from AAO hard templates

Self-ordered AAO is characterized by regular hexagonal arrays of parallel pores with sharp pore size distributions. Lattice constants and pore diameters are adjustable to values between a few tens of nanometres and a few hundreds of nanometres. The pore depths can be tuned in the range from a few hundreds of nm to several hundreds of μm , thus allowing the precise adjustment of the aspect ratios of the nanorods prepared by replicating the pores. Well-designed geometries as those imposed by self-ordered AAO hard templates are the prerequisite for retaining

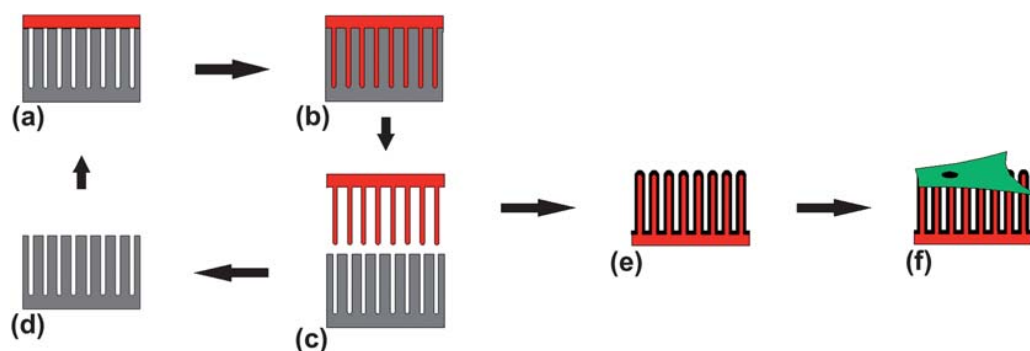


Fig. 1 Nondestructive fabrication of nanorod-based ECMs using recyclable AAO hard templates. (a) PDLLA is heated on top of the AAO; (b) PDLLA infiltrates the pores, thus forming an array of PDLLA nanorods connected with a continuous PDLLA film on top of the AAO hard templates; (c) the PDLLA nanorods are detached from the AAO hard templates; (d) the AAO hard template is ready for reuse; (e) the released PDLLA nanorod arrays are coated with heparin/gelatin and (f) used for cell culturing.

the structural integrity of nanorod arrays under the conditions of cell culturing. We produced PDLLA nanorod arrays using self-ordered AAO with a pore diameter of 180 nm, a pore depth of 600 nm or 1 μm and a lattice constant of 500 nm. The AAO was attached to underlying aluminium substrates so that the pore bottoms were closed. The AAO hard templates were modified with 1*H*,1*H*,2*H*,2*H*-perfluorodecyl-trichlorosilane in order to minimize adhesion between the rods formed within the pores and the pore walls. To infiltrate the PDLLA, it was melted on top of the AAO at 523 K (Fig. 1a). The perfluorated silane rendered the initially hydroxyl-terminated high-energy surfaces of the pore walls into low-energy surfaces so that spontaneous infiltration of the PDLLA driven by adhesion was prevented. However, the PDLLA readily moved into the pores if the AAO was gently pressed against the heated PDLLA. The PDLLA nanorod arrays thus formed were connected to a PDLLA film located on top of

the hard templates (Fig. 1b). Mechanical extraction^{28,29} of the PDLLA nanorods from the AAO moulds allows circumventing the destruction of the latter by wet-chemical etching with bases (Fig. 1c). Therefore, the detached AAO hard templates can be reused (Fig. 1d), which is a prerequisite for the up-scaling of the template-based fabrication of nanorod arrays. In three successive molding cycles, each of which yielded a PDLLA nanorod array, no noticeable damage to the AAO hard templates occurred.

PDLLA nanorod arrays with areas up to 9 cm² (Fig. 2a) were thus obtained and bioactivated with a heparin/gelatin mixture (weight ratio heparin/gelatin 30 : 70) (Fig. 1e) to promote interactions between cells and the PDLLA nanorods. Heparin is a linear polysaccharide consisting of repeating units of 1 \rightarrow 4-linked pyranosyluronic acid and 2-amino-2-deoxyglucopyranose (glucosamine) residues that has the highest negative charge density of any known natural macromolecule.³⁰ The high charge density of heparin and its pronounced tendency to form ionic complexes and hydrogen bonds result in strong interactions with a broad range of proteins and cells. More specifically, heparin modulates the biological activity of the transforming growth factor TGF- β 1, which plays an important role in cell migration and proliferation, and consequently in the performance of ECMs.³¹ Gelatin, which is a major component of connective tissue, improves biocompatibility.³² Coating the PDLLA nanorods with heparin/gelatin increased their diameters from about 180 nm to about 220 nm, but their local hexagonal arrangement imposed by the AAO hard template was still retained (Fig. 2b). The thickness of the heparin/gelatin coating amounted to a few tens of nanometres only. Since much higher amounts of both materials occur under typical physiological conditions in natural ECMs, it is reasonable to assume that the heparin/gelatin coating does not significantly influence bioresorption and biodegradation.

To combine well-defined surface topography with mechanical stability under real-life conditions, a relatively large spacing of 280 nm between the PDLLA nanorods even after their activation with the heparin/gelatin coating was combined with relatively low aspect ratios ranging from 3 to 5. The characteristic dimensions of the PDLLA nanorods and the spacing between them was about two orders of magnitude smaller than the typical size of the fibroblast cells cultured on the PDLLA nanorod arrays (Fig. 1f).

Cell growth and cell interactions on PDLLA nanorod arrays extracted from AAO hard templates

To study the morphology of single cells, we cultured fibroblasts for one day on a heparin/gelatin-functionalized PDLLA nanorod array extracted from AAO. As obvious from Fig. 3, even after exposure to the culture medium and the seeding of cells the heparin/gelatin functionalized nanorods did not collapse so that the arrays they constituted remained intact. Thus, well spread fibroblasts exhibiting the characteristic elongated morphology typically occurring in tissue were obtained. The representative SEM image seen in Fig. 3a shows a fibroblast with an aspect ratio (length divided by width) of about 3. The large number of filopodia protruding from the cell along its entire perimeter is a signature of pronounced biological activity, cell proliferation and specific cell/matrix interactions. The detail displayed in

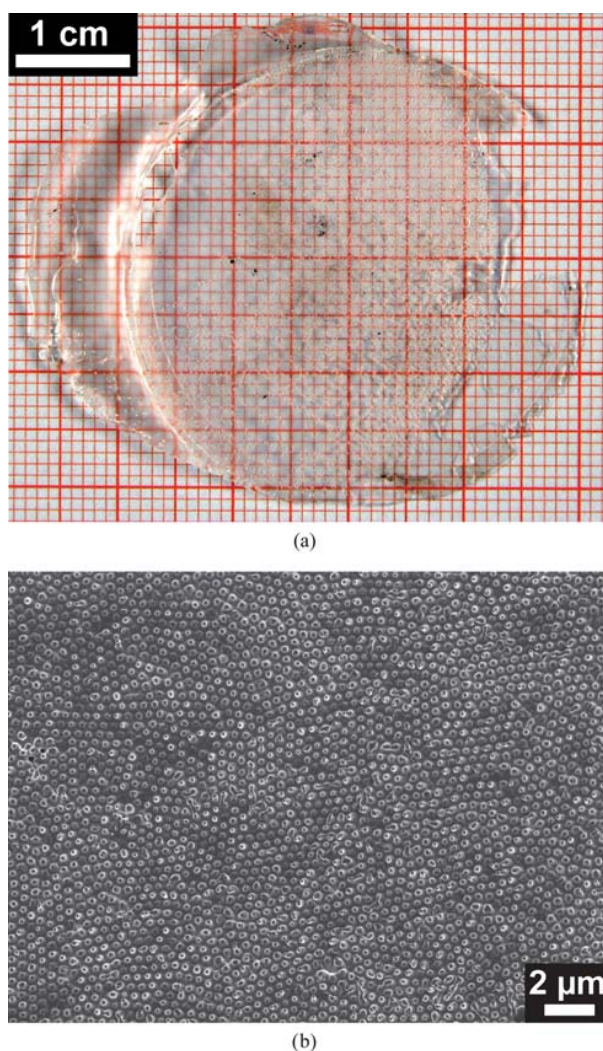


Fig. 2 (a) Photograph of a PDLLA nanorod array released from AAO (pore diameter: 180 nm, pore depth: 1 μm , lattice constant: 500 nm) by ripping it off with tweezers. (b) Scanning electron microscopy (SEM) image of a PDLLA nanorod array after nondestructive release from AAO (pore diameter 180 nm; pore depth 1 μm ; lattice constant 500 nm) and functionalization with heparin/gelatin.

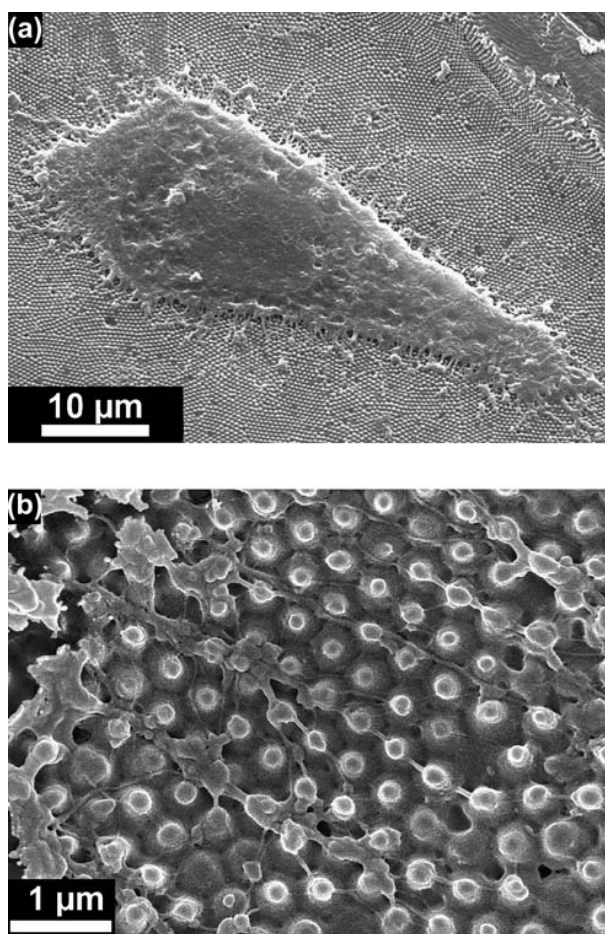


Fig. 3 SEM images of a single fibroblast cell from human skin on heparin/gelatin-functionalized PDLLA nanorod arrays extracted from AAO (pore diameter: 180 nm; pore depth: 1 µm; lattice constant: 500 nm) obtained by culturing for one day: (a) Large-field view and (b) detail showing filopodia protruding from the cell body.

Fig. 3b reveals that thick filopodia with diameters of ~ 100 nm occur close to the cell body, which split into thinner filopodia with diameters of ~ 50 nm. The thinner filopodia are predominantly attached to the tips of the heparin/gelatin-functionalized PDLLA nanorods. This behavior is consistent with the biological function of heparin as an activator agent of the cells transforming the growth factor TGF-B1. It is obvious that the fibroblast cell seen in Fig. 3 recognizes the nanorod array as a rough surface providing the heparin/gelatin-functionalized PDLLA nanorods as well-defined topographic cues sensed by the filopodia. After culturing for 4 days, heparin/gelatin-functionalized PDLLA nanorod arrays with edge lengths of ~ 3 mm were almost completely covered by a dense layer of fibroblast cells that showed excellent viability while retaining a highly elongated morphology (Fig. 4a). The elongated morphology of the fibroblasts is obvious from the SEM top view image seen in Fig. 4b. Even after culturing for four days the hexagonal arrangement of uncovered heparin/gelatin-functionalized PDLLA nanorods near the edges of the fibroblast layers was conserved (Fig. 4c).

A representative laser confocal fluorescence microscopy image of a fibroblast layer on a heparin/gelatin-functionalized PDLLA

nanorod array obtained by culturing for four days is seen in Fig. 5. The blue spots are the nuclei of the cells stained with Hoechst 33342, whereas red color indicates the presence of actin filaments stained with phalloidin. Actin is one of the three major components of the cytoskeleton, and thin actin filaments are components of the contractile apparatus in cells. Thus, actin is involved in many important cellular processes including cell motility, cell division and cytokinesis, vesicle and organelle movement as well as cell signaling and in the establishment and maintenance of cell junctions and cell shape. The presence of actin throughout the entire cell body and the occurrence of filopodia are indicative of the excellent adhesion of the fibroblasts to the heparin/gelatin-functionalized PDLLA nanorod arrays. The fibroblasts are aligned on a local scale, and they have highly elongated shapes with aspect ratios of about 3 to 5.

Cell growth and cell interactions on PDLLA microrod arrays extracted from macroporous silicon hard templates

The importance of feature sizes and mechanical stability of the substrates is obvious from the results obtained by culturing fibroblasts on PDLLA microrod arrays extracted from macroporous silicon.²⁷ The macroporous silicon hard templates contained pores 1 µm in diameter and 10 µm in depth arranged in a square lattice with a lattice constant of 2 µm. The heparin/gelatin coated PDLLA microrods thus obtained with a length of 10 µm and a diameter of ~ 1.3 µm can be considered as models for bunches of condensed PDLLA nanorods (Fig. 6). Some of the microrods were stretched or contained neck-like segments resulting from shear forces occurring during extraction.

Fig. 7a shows a representative fluorescence microscopy image of fibroblasts after culturing for two days on a PDLLA microrod array released from macroporous silicon. The fibroblasts had aspect ratios of 1 to 2 and were, therefore, much more isotropic than those seeded on heparin/gelatin functionalized PDLLA nanorod arrays released from AAO. Moreover, the cells did not show clear orientation or local alignment. In striking contrast to the heparin/gelatin functionalized PDLLA nanorod arrays extracted from AAO, even after culturing for four days only single, separated cells grown around individual heparin/gelatin functionalized PDLLA microrods were found (Fig. 7b). Therefore, increasing the characteristic feature sizes of the rod arrays by a factor of four led to dramatic changes in the cell/matrix interactions. The cells recognized heparin/gelatin functionalized PDLLA microrod arrays as a quasi-three dimensional scaffold rather than as a surface providing cues for cell adhesion, such as in the case of the heparin/gelatin functionalized PDLLA nanorod arrays extracted from AAO. As compared to the latter, cell proliferation on PDLLA microrod arrays extracted from macroporous silicon was significantly impeded.

Experimental

Self-ordered AAO and macroporous silicon were prepared according to procedures described elsewhere.^{24–27} To silanize the hard templates, the AAO was at first treated with a 30 wt% solution of hydrogen peroxide at 50 °C for 2 h, rinsed with deionized water and dried at 120 °C for 15 minutes, whereas macroporous silicon was treated with 5% hydrofluoric

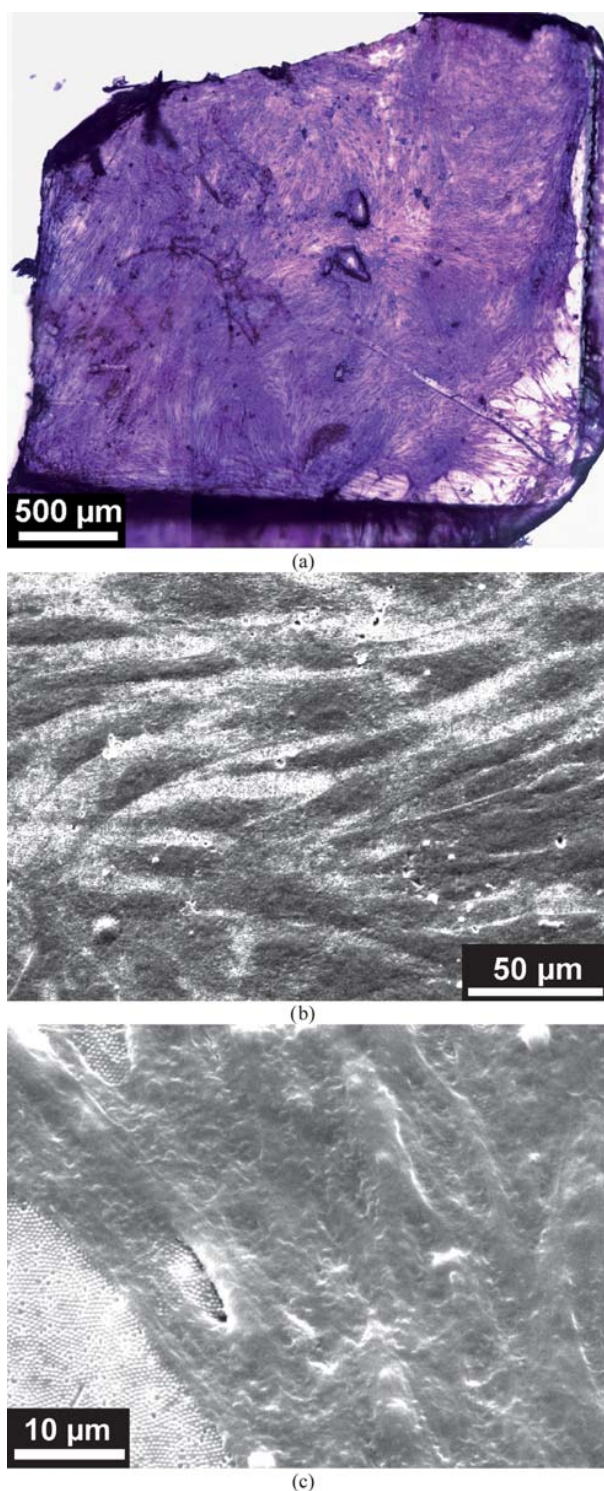


Fig. 4 Tissue obtained by culturing fibroblasts from human skin for four days on heparin/gelatin-functionalized PDLLA nanorod arrays with an edge length of about 3 mm extracted from AAO (pore diameter: 180 nm; lattice constant: 500 nm). (a) Collage of optical microscopy images displaying cells fixated with glutaraldehyde and incubated with 100 μl of a solution of 1 mg ml^{-1} crystal violet in phosphate buffer (pH 7.2). The PDLLA nanorods were extracted from AAO with a pore depth of 600 nm. (b) and (c) SEM images of tissue

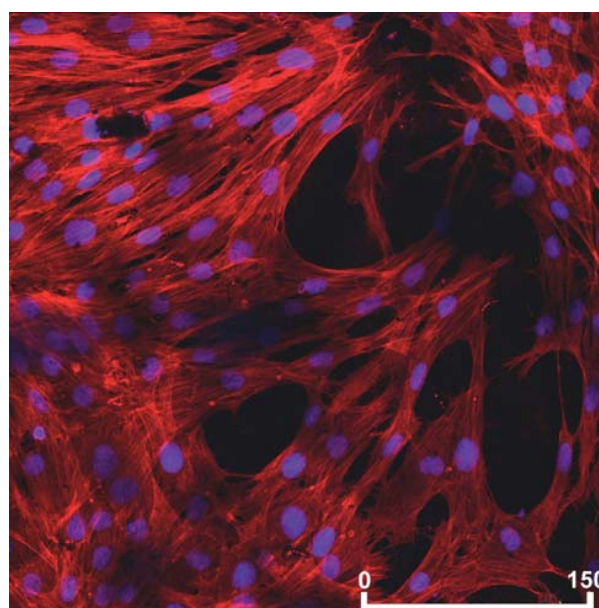


Fig. 5 Laser confocal microscopy image of fibroblasts on PDLLA nanorods extracted from AAO (pore diameter 180 nm; pore depth 1 μm , lattice constant 500 nm) obtained by culturing for four days. The cells were fixated with formaldehyde and stained. The nuclei are blue and the presence of actin filaments is indicated by red color.

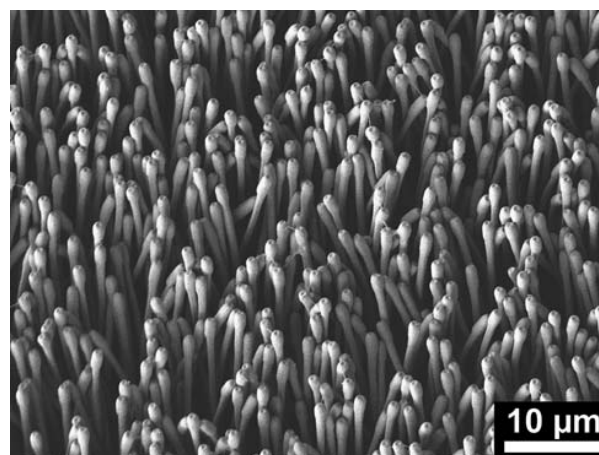


Fig. 6 SEM image of a PDLLA microrod array after nondestructive release from macroporous silicon (pore diameter 1 μm ; pore depth 10 μm ; lattice constant 2 μm) after functionalization with heparin/gelatin.

acid solution for 1 h at room temperature, rinsed with deionized water, boiled in a mixture containing 30 vol% sulfuric acid and 70 vol% of a 30 wt% hydrogen peroxide solution for 1 h, and then rinsed with deionized water and ethanol. Both macroporous Si and AAO were then placed in a furnace at 90 $^{\circ}\text{C}$ for 3 h and at 130 $^{\circ}\text{C}$ for another 3 h in the presence of 0.05 ml

layers on PDLLA nanorod arrays extracted from AAO with a pore depth of 1 μm .

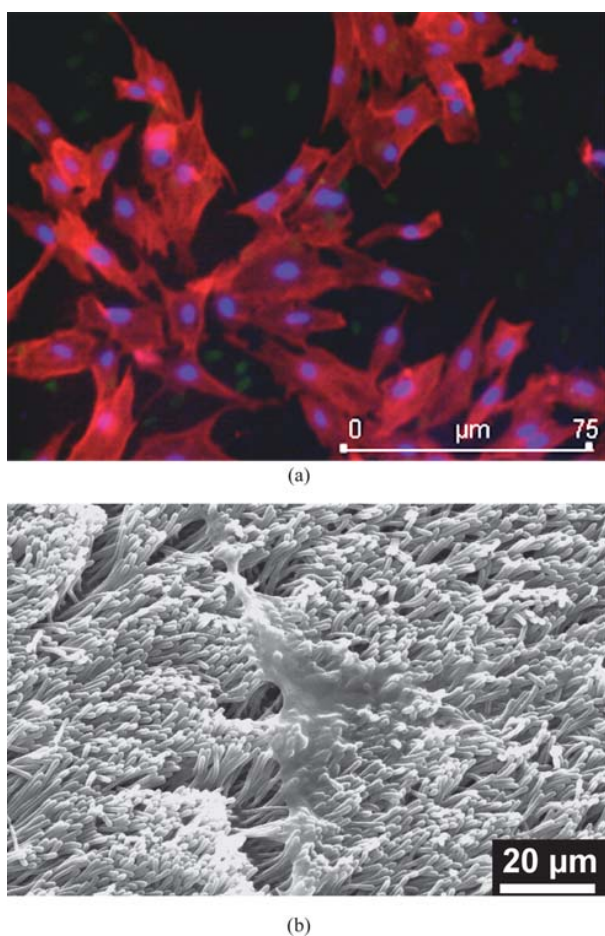


Fig. 7 Fibroblasts from human skin cultured on heparin/gelatin-functionalized PDLLA microrod arrays extracted from macroporous silicon (pore diameter: 1 μm ; pore depth: 10 μm ; lattice constant: 2 μm). (a) Fluorescence microscopy image obtained after culturing for two days. The fibroblasts were stained in the same way as the cells seen in Fig. 5. (b) SEM image after culturing for four days.

1*H*,1*H*,2*H*,2*H*-perfluorodecyl-trichlorosilane ($\text{C}_{10}\text{H}_4\text{Cl}_3\text{F}_{17}\text{Si}$; 97%; purchased from Aldrich).

The infiltration of PDLA (Resomer R207, Boehringer Ingelheim) was carried out as follows. The surface-modified hard templates were placed on a hotplate and heated to 523 K. The PDLA was melted on top of the hard templates for 5 minutes and then gently pressed against their surface. We mounted the hard templates containing the PDLA rods on a home-made apparatus with a fixed and a movable stud. The PDLA film on top of the templates was glued on the fixed stud and the underside of the hard templates on the movable stud. The movable stud was driven by a dc motor (8000 rpm) combined with a reduction gear (975:1) so that a force perpendicular to the surface of the template was applied. Alternatively, the PDLA rod arrays were torn off with tweezers. An aqueous solution containing 1.5 wt% of a mixture of 30 wt% heparin and 70 wt% gelatin was spin coated on the PDLA nanorod arrays at 500 rpm for 30 seconds, then at 2000 rpm for another 30 seconds and finally at 3000 rpm for 50 seconds. This spin coating

sequence was repeated three times to dry the samples. Subsequently, the functionalized PDLA rod arrays were exposed to a saturated glutaraldehyde atmosphere at room temperature for 12 h to crosslink the initially water-soluble heparin/gelatin layer.³³

Human dermal fibroblasts (type DPK-SKDF-HS, Dominion Pharmakine, Spain) were cultured at 37 $^{\circ}\text{C}$ in humidified air in the presence of 5% CO_2 . As culture medium, Dulbecco's Modified Eagle's Medium (DMEM, Sigma) supplemented with 10 vol% fetal bovine serum (FBS, Gibco), 2 vol% L-glutamine (Sigma) and 1 vol% penicillin/streptomycin (100 UI/ml, 100 $\mu\text{g}/\text{ml}$; Sigma) was used. Sterilized heparin/gelatin-functionalized PDLA nanorod arrays were placed in a 96 well-plate, seeded with fibroblasts at 8×10^4 cells per ml and kept at 37 $^{\circ}\text{C}$ in the presence of 5% CO_2 for 1 to 4 days. For SEM investigations the cells were fixated with a solution of 2.5 vol% glutaraldehyde in deionized water for two hours at room temperature. For characterization by laser confocal fluorescence microscopy and fluorescence microscopy the cells were fixated with a solution of 3.4 vol% formaldehyde in PBS (phosphate buffer saline, pH 7.2) for 1 h, washed with PBS, permeabilized with 0.5% triton in PBS for 20 min, and washed with 0.1% Tween 20 in PBS. The nuclei were stained with an 8×10^{-5} molar solution of the blue fluorescent dye Hoechst 33342, and actin filaments were stained with a 4×10^{-7} molar solution of the red staining agent phalloidin.

Conclusions

Biodegradable ECMs consisting of mechanically stable arrays of aligned polylactide nanorods extending up to 9 cm^2 were prepared by nondestructive extraction from recyclable self-ordered AAO hard templates, an approach combining the advantages of top-down lithography (well-defined topography) and self-assembly (low costs, high throughput, feature size in the 100 nm range). Pore diameter, pore depth and period of the self-ordered AAO hard templates are handles to adjust the properties of the nanorod arrays obtained as their faithful replicas. On arrays of heparin/gelatin functionalized nanorods with diameters of the order of 220 nm and aspect ratios ranging from 3 to 5, which had an array period of the order of 500 nm, fibroblasts formed dense tissue layers, showed excellent adhesion and exhibited a highly elongated morphology such as in natural tissue. On arrays of microrods with diameters of $\sim 1.3 \mu\text{m}$ and aspect ratios of ~ 8 , which have an array period of 2 μm , the fibroblasts were significantly less elongated and their proliferation was significantly reduced. This outcome indicates that not only the design of ECM features on subcellular length scales but also their stability under real life conditions is a crucial prerequisite for specific cell/matrix interactions.

Self-ordered AAO hard templates do not only allow fabrication of mechanically stable biodegradable nanorod arrays by faithful replication of the nanopore arrays they contain, provided pore diameters, interpore spacing and pore depth are properly selected. The use of rigid and thermally-stable AAO hard templates will also enable control over structure formation processes in the nanorods, such as crystallization, mesophase formation and phase separation, to adjust their mechanical properties or to implement specific functionalities such as controlled drug release.

Acknowledgements

Technical support from S. Kallaus, K. Sklarek and D. Gómez, the donation of Resomer R207® by Boehringer Ingelheim, as well as financial support from the CICYT (projects MAT2005-0179 and MAT2007-63355) and from the German Research Foundation (Priority Program 1420, STE 1127/12-1) are gratefully acknowledged. S. G. thanks the German Academic Exchange Service (DAAD) for a fellowship and M. F. the Ramón y Cajal Program for support.

Notes and references

- 1 C. Kumar, *Nanotechnologies for the Life Science, Vol. 9: Tissue, Cell and Organ Engineering*, Wiley-VCH, Weinheim, Germany, 2006, Ch. 1, pp. 1–56.
- 2 A. Curtis and C. Wilkinson, *Biomaterials*, 1997, **18**, 1573.
- 3 J. J. Norman and T. A. Desai, *Ann. Biomed. Eng.*, 2006, **34**, 89.
- 4 M. J. Dalby, M. O. Riehle, H. Johnstone, S. Affrossman and A. S. G. Curtis, *Cell Biol. Int.*, 2004, **28**, 229.
- 5 M. J. Dalby, M. O. Riehle, S. D. Sutherland, A. Hossein and A. S. G. Curtis, *Biomaterials*, 2004, **25**, 5415.
- 6 W. J. Li, C. T. Laurencin, E. J. Caterson, R. S. Tuan and F. K. Ko, *J. Biomed. Mater. Res.*, 2002, **60**, 613.
- 7 J. A. Matthews, G. E. Wnek, D. G. Simpson and G. L. Bowlin, *Biomacromolecules*, 2002, **3**, 232.
- 8 R. Murugan and S. Ramakrishna, *Tissue Eng.*, 2007, **13**, 1845.
- 9 J. Xie, X. Li and Y. Xia, *Macromol. Rapid Commun.*, 2008, **29**, 1775.
- 10 C. P. Barnes, S. A. Sell, E. D. Boland, D. G. Simpson and G. L. Bowlin, *Adv. Drug Delivery Rev.*, 2007, **59**, 1413.
- 11 C.-H. Choi, S. H. Hagvall, B. M. Wu, J. C. Y. Dunn, R. E. Beygui and C. J. Kim, *Biomaterials*, 2007, **28**, 1672.
- 12 W. H. Roos, A. Roth, J. Konle, H. Presting, E. Sackmann and J. P. Spatz, *ChemPhysChem*, 2003, **4**, 873.
- 13 T. Steinberg, S. Schulz, J. P. Spatz, N. Grabe, E. Mussig, A. Kohl, G. Komposch and P. Tomakidi, *Nano Lett.*, 2007, **7**, 287.
- 14 A. Saez, M. Ghibaudo, A. Buguin, P. Silberzan and B. Ladoux, *Proc. Natl. Acad. Sci. U. S. A.*, 2007, **104**, 8281.
- 15 S. Nomura, H. Kojima, Y. Ohyabu, K. Kuwabara, A. Miyauchi and T. Uemura, *Jpn. J. Appl. Phys.*, 2005, **44**, L1184.
- 16 D.-H. Kim, P. Kim, I. Song, J. M. Cha, S. H. Lee, B. Kim and K. Y. Suh, *Langmuir*, 2006, **22**, 5419.
- 17 A. Mahdavi, L. Ferreira, C. Sundback, J. W. Nichol, E. P. Chan, D. J. D. Carter, C. J. Bettinger, S. Patanavanich, L. Chignozha, E. Ben-Joseph, A. Galakatos, H. Pryor, I. Pomerantseva, P. T. Masiakos, W. Faquin, A. Zumbuehl, S. Hong, J. Borenstein, J. Vacanti, R. Langer and J. M. Karp, *Proc. Natl. Acad. Sci. U. S. A.*, 2008, **105**, 2311.
- 18 C. R. Martin, *Science*, 1994, **266**, 1961.
- 19 M. Steinhart, *Adv. Polym. Sci.*, 2008, **220**, 123.
- 20 S. L. Tao and T. A. Desai, *Nano Lett.*, 2007, **7**, 1463.
- 21 C. Y. Hui, A. Jagota, Y. Y. Lin and E. J. Kramer, *Langmuir*, 2002, **18**, 1394.
- 22 Y. Zhang, C.-W. Lo, J. A. Taylor and S. Yang, *Langmuir*, 2006, **22**, 8595.
- 23 J. Kong, K.-L. Yung, Y. Xu, L. He, K. H. Lau and C. Y. Chan, *J. Polym. Sci., Part B: Polym. Phys.*, 2008, **46**, 1280.
- 24 H. Masuda and K. Fukuda, *Science*, 1995, **268**, 1466.
- 25 H. Masuda, K. Yada and A. Osaka, *Jpn. J. Appl. Phys., Part 2*, 1998, **37**, L1340.
- 26 M. Steinhart, P. Göring, H. Dernaika, M. Prabhakaran, U. Gösele, E. Hempel and T. Thurn-Albrecht, *Phys. Rev. Lett.*, 2006, **97**, 027801.
- 27 V. J. Lehmann, *J. Electrochem. Soc.*, 1993, **140**, 2836.
- 28 S. Grimm, K. Schwirn, P. Göring, H. Knoll, P. T. Miclea, A. Greiner, J. H. Wendorff, R. B. Wehrspohn, U. Gösele and M. Steinhart, *Small*, 2006, **3**, 993.
- 29 S. Grimm, R. Giesa, K. Sklarek, A. Langner, U. Gösele, H.-W. Schmidt and M. Steinhart, *Nano Lett.*, 2008, **8**, 1954.
- 30 I. Capila and R. J. Linhardt, *Angew. Chem., Int. Ed.*, 2002, **41**, 390.
- 31 M. A. Palladino, R. E. Morris, H. F. Starnes and A. D. Levinson, *Ann. N. Y. Acad. Sci.*, 1990, **593**, 181.
- 32 Y. Lin, X. Chen, X. Jing, Y. Jiang and Z. Su, *J. Appl. Polym. Sci.*, 2008, **109**, 530.
- 33 N. Reddy, Y. Tan, Y. Li and Y. Yang, *Macromol. Mater. Eng.*, 2008, **293**, 614.